Practical Considerations

We note that the equations for the weighting factors Eqs. (19) and (22) involve the additional unknown variables J_{cccc} and J_{ccccc}. In practice, we assert that the function $J(c, s)$ is representable in the form $a_0(s) + a_1(s)c + a_2(s)c^2 + a_3(s)c^3$ in the neighborhood of the optimal estimate e_s. This makes J_{cccc} and J_{ccccc} negligible in the neighborhood of e_s. In this case, the estimator equations are

$$de_s/ds = g(e_s, s) + \sigma(e_s, s)\sigma_c(e_s, s) + p_s\sigma^2(e_s, s) + q_s(y_s - e_s) \quad (15)$$

$$dq_s/ds = 2g_c q - q^2 - 2\sigma^2 qp^2 + 2\sigma\sigma_c pq + (\sigma_c^2 + \sigma\sigma_{cc})q - 2pq^2(y - e) \quad (23)$$

and

$$dp_s/ds = pq^{-1}(dq/ds) - \tfrac{3}{2}g_{cc} - 3pq^{-1}(g_c + \sigma_c^2 + \sigma\sigma_{cc}) - 2(3\sigma_c\sigma_{cc} + \sigma\sigma_{ccc})q^{-1} \quad (24)$$

Multichannel Filtering

Here we consider a vector system described by Eqs. (1) and (2), where x and g are n-vectors, β is an r-vector Brownian motion, and σ is an $n \times r$ matrix. The observation is described by Eq. (3), where y and h are m-vectors with $m \leq n$.

As before, we wish to find an estimate e_s of x_s based on the observation $0_s = \{y_t, 0 \leq t \leq s\}$ such that Eq. (5) holds for all functionals $c = (c_1, \ldots, c_n)'$ of 0_s with probability one. The derivation of the estimator equations is analogous to that in the above scalar case. Hence, it will not be elaborated here. We will simply display the estimator equations in the following:

$$de_s/ds = g(e_s, s) + q_s h_c'(e_s, s)[y_s - h(e_s, s)] + \tfrac{1}{4}q_s[\text{trace}(A_{c_1}B + AB_{c_1}), \ldots, \text{trace}(A_{c_m}B + AB_{c_m})]' \quad (25)$$

$$dq_s/ds = -\tfrac{1}{2}q_s\{2h_{cc}Qh + 2h_c'Qh_c - 2h_{cc}Qy - J_{ccc}g - 2q^{-1}g_c - 2g_c'q^{-1} - \tfrac{1}{2}[\text{trace}(A_{c_ic_j}B + AB_{c_ic_j})]\}q_s - 2q(J_{c_ic_jc}(de_s/ds))q \quad (26)$$

where $A = \sigma\sigma'$ and $B = J_{cc}$.

Under the assumption that $J(c, t)$ is representable in the quadratic form of c, the estimator equations are displayed as follows:

$$de_s/ds = g(e_s, s) + q_s h_c'(e_s, s)Q(s)[y_s - h(e_s, s)] + \tfrac{1}{4}q_s(\text{trace } 4\sigma_{c_1}\sigma' q_s^{-1}, \ldots, \text{trace } 4\sigma_{c_m}\sigma' q_s^{-1})' \quad (27)$$

and

$$dq_s/ds = q_s h_{cc}(e_s, s)Q(s)[y_s - h(e_s, s)] + g_c(e_s, s)q_s + q_s g_c'(e_s, s) - q_s h_c'(e_s, s)Q(s)h_c(e_s, s)q_s + \tfrac{1}{4}[\text{trace } 4(\sigma_{c_ic_j}\sigma' q^{-1} + \sigma_{c_i}\sigma_{c_j}q_s^{-1})]q_s \quad (28)$$

References

[1] Bellman, R. E., Kagiwada, H. H., Kalaba, R. E., and Sridhar, R., "Invariant Imbedding and Nonlinear Filtering Theory," *Journal of the Astronautical Sciences*, Vol. 13, 1966, pp. 110–115.

[2] Detchmendy, D. M. and Sridhar, R., "Sequential Estimation and States and Parameters in Noisy Nonlinear Dynamical Systems," *Transactions of the ASME*: *Journal of Basic Engineering*, Vol. 88, 1966, pp. 362–368.

[3] Bass, R. W., Norum, V. D., and Schwartz, L., "Optimal Multichannel Nonlinear Filtering," *Journal of Mathematical Analysis and Applications*, Vol. 16, 1966, pp. 162–164.

[4] Ito, K., "On Stochastic Differential Equations," *Memoirs American Mathematical Society*, Vol. 4, 1951.

[5] Maruyama, G., "Continuous Markov Processes and Stochastic Equations," *Rendiconti del Circolo Matematico di Palermo* (2), Vol. 4, 1955, pp. 48–90.

Population Inversion of Atomic Carbon in Recombining Plasma Flow

S. W. Bowen*
University of Michigan, Ann Arbor, Mich.

AND

C. Park†
NASA Ames Research Center, Moffett Field, Calif.

Introduction

RECENT theoretical calculations[1] and experimental measurements[2] have indicated that a large overpopulation of the upper neutral atom excited states with respect to the ground state can exist in an arc-heated plasma expanding through a nozzle. In Ref. 2, it is shown experimentally that such an overpopulation results ultimately in a population inversion between a pair of states corresponding to a visible or infrared spectral line. In Ref. 1, it is predicted that a population inversion may occur also for an ultraviolet line. The purpose of the present work is to examine experimentally the population inversion of an ultraviolet line. Here, spectroscopic measurements made on high-pressure high-temperature, arc-heated helium-methane or argon-methane mixtures expanding through a nozzle show a population inversion in the neutral carbon line at 2478.6 Å corresponding to the $2p^2\,{}^1S_0 \rightarrow 2p\,3s\,{}^1P_1{}^0$ transition.

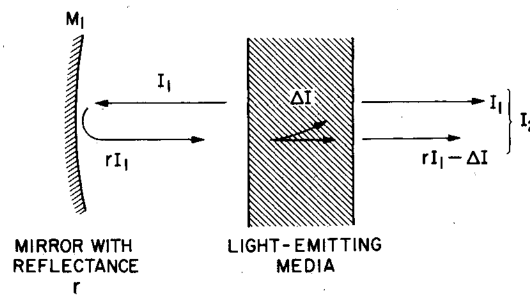

Fig. 1 Schematic of the single reflection absorption measurement.

Theory

In Ref. 1, the possibility of population inversion for a neutral nitrogen atom line at 1745 Å was indicated. Although such a possibility does exist, it is difficult to verify experimentally because the wavelength is within the vacuum ultraviolet range. A line transition similar to 1745 NI exists, however, in neutral carbon at 2478.6 Å which is in the quartz-ultraviolet wavelength region.

The population inversion for any spectral line can be observed by measuring the apparent absorption coefficient of the line. This is done by placing a concave mirror of reflectance r behind the plasma (see Fig. 1). If I_1 is the direct plasma

Presented as Paper 71-592 at the AIAA 4th Fluid and Plasma Dynamics Conference, Palo Alto, Calif., June 21–23, 1971; submitted July 26, 1971; revision received November 11, 1971. Work performed at the Ames Research Center in part under a cooperative program between the University of Santa Clara and Ames Research Center while the senior author was a Visiting Assistant Professor, University of Santa Clara, Santa Clara, Calif. and partly under a NASA-ASEE Summer Faculty Fellowship.

Index categories: Atomic, Molecular, and Plasma Properties; Thermochemistry and Chemical Kinetics; Nozzle and Channel Flow.

* Assistant Professor. Department of Aerospace Engineering. Member AIAA.

† Research Scientist. Member AIAA.

radiance with a mirror M_1 covered and I_2 is the sum of the direct emission and the partially absorbed emission, then

$$I_2 = I_1 + rI_1 - \Delta I \tag{1}$$

where ΔI is the radiance absorbed within the plasma. The line absorption A_L defined as the ratio of the absorbed to the incident radiance[3,4] is given by

$$A_L = \Delta I/(rI_1) = (1 + r - I_2/I_1)/r \tag{2}$$

Because the spectrograph spectral band pass is usually large compared with the line width, I_1 and I_2 are radiances integrated over the entire line profile and path length.

The observed line absorption coefficient, Eq. (2), can be related to the population densities of the upper and the lower states of the line concerned as follows. From the radiative transfer theory[3,4] one can show for a homogeneous path of length L that the integrated line absorption A_L can be written in terms of atomic parameters as[5]

$$A_L = 2 - \int_{\text{line}} [1 - \exp(-2\kappa_\nu{}^* L)]\, d\nu \Big/ \int_{\text{line}} [1 - \exp(-\kappa_\nu{}^* L)]\, d\nu \tag{3}$$

where $\kappa_\nu{}^* = \alpha_0 N_l{}^* H(a,u) = \kappa_0{}^* H(a,u)$ is the linear absorption coefficient corrected for stimulated emission. The quantity α_0 is the absorption cross section at the center of a pure Doppler line, $H(a,u)$ is the Voigt function[6,7] and $N_l{}^* = N_l[1 - (N_u/g_u)/(N_l/g_l)]$ is the effective lower state density. The integrals in Eq. (3) can be evaluated in terms of the equivalent width.[7] For the experimental conditions of interest $a \ll 1$ so that the Doppler limit for the Voigt function applies, i.e., $H(a,u) = \exp(-u^2)$. For optical depths $\kappa_0{}^* L \ll 1$, Eq. (3) yields

$$A_L = \kappa_0{}^* L/2^{1/2} \tag{4}$$

Formulas giving A_L for larger $\kappa_0{}^* L$ are given by Mitchell and Zemansky.[3]

Comparing Eqs. (4) and (2), we note if $\Delta I > 0$ ordinary absorption processes dominate over the stimulated emission, and $A_L > 0$, whereas if $\Delta I < 0$, a population inversion has occurred and $A_L < 0$.

Equipment and Measurements

The measurements are conducted in the freejet stream produced in a constricted-arc, plasma-jet wind tunnel of 1.27-cm constrictor diameter at Ames Research Center. The contoured nozzle is approximately 25 cm long and has an exit diameter of 5.95 cm. The measurements are made 11 cm downstream of the exit plane. Since the wind-tunnel nozzle operates in a highly underexpanded mode, an abrupt expansion takes place within the 11 cm distance between the nozzle exit plane and the measured station. The area ratio at the test station is approximately 50. The diameter of the plasma-jet stream at the measuring station is of the order of 10 cm, of which approximately 5 cm is considered to contain the hot plasma core. A mixture of helium and methane or argon and methane is used as the working gas, and the methane content is of the order of 5% by mole. The methane dissociates within the arc-heater and provides the atomic carbon.

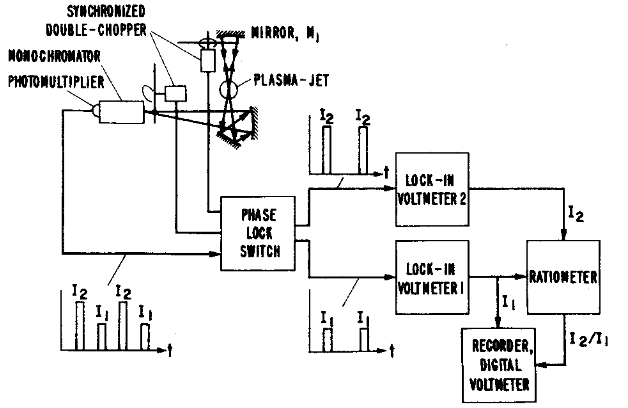

Fig. 2 Schematic of the single-pass measuring technique to determine I_2/I_1 from plasma.

The measurement of I_1 and I_2 in Eq. (2) is performed by using the mirror-chopper system shown in Fig. 2. As shown in the figure, it consists of two spherical mirrors, a Brower Model 1513 ratiometer system having two phase-locked choppers, two lock-in voltmeters, and the ratiometer, together with a digital voltmeter and a two-channel recorder. This system provides both the separately time-averaged signals I_1 and I_2 and their ratio. The over-all repetition frequency was approximately 20 Hz, with a typical signal averaging time of 3 sec, thus resulting in a well-stabilized signal of high signal-to-noise ratio. The precision of the intensity ratio I_2/I_1, set mainly by the arc tunnel unsteadiness, is ± 0.005. The radiance was measured using a 1/2 meter scanning monochromator having a reciprocal dispersion of 17.5 amp/mm. A Hitachi R106 ultraviolet sensitive photomultiplier tube was used as the light detector. Slit widths were varied between 0.05 and 0.3 mm.

In addition to the ratio I_2/I_1, one must know the mirror reflectance r at 2479 Å in order to determine the absorption A_L by Eq. (2). The value of r is crucial, since a small uncertainty in r will seriously affect the magnitude and sign of A_L, as is apparent from the form of Eq. (2). Three different methods were employed to determine the mirror reflectance at the required wavelength.[5] The first method observed the optically thin continuum near the line setting $\Delta I = 0$ in Eq. (2); the second used the initially thin carbon line itself as the mole fraction of carbon is increased; the third used a beamsplitter and light source. All three methods gave a value of $r = 0.58$ at 2479 Å for the mirror M_1.

Results

Experimental values obtained in both helium-methane and argon-methane plasmas are shown in Table 1. Numbers 1–7 are helium-methane runs, while 8 and 9 are argon-methane runs. The largest absolute value of A_L is that for run number 5.

These values of A_L give fairly large population inversions. Estimates of the test section conditions[5] give $N_e \approx 10^{14}$ cm^{-3}

Table 1 Experimental conditions, measured integrated line absorption and optical depths of CI 2478.6 Å line

Number	Mole fraction carbon	Cathode pressure, atm	Total mass flow, g/sec	Enthalpy, M_j/Kg	$(\Delta I/rI_1) = A_L$	$\kappa_0{}^* L$
1	0.051	3.0	2.2	140	−0.362	−0.42
2	0.051	3.0	2.1	210	−0.276	−0.33
3	0.051	3.0	2.1	210	−1.57	−1.20
4	0.067	2.72	2.1	130	−1.10	−0.96
5	0.033	4.75	2.5	190	−2.24	−1.46
6	0.080	2.38	1.9	140	−1.90	−1.33
7	0.031	1.97	1.6	140	−1.10	−0.96
8	0.03	2.05	5.0	40	−0.845	−0.80
9	0.03	3.05	6.0	50	−0.845	−0.80

and $T_e = 3500\,^\circ$K with the pressure and heavy particle temperature being 1 torr and $1000\,^\circ$K, respectively. The value of $a \approx 10^{-3}$. Using the atomic constants for the CI 2479 line given in Ref. 8, Eq. (3) gives $\kappa_0{}^*L = -1.46$ for Run 5. Assuming a path length $L = 5$ cm, the carbon atom density is $\approx 3.3 \times 10^{14}$ cm^{-3} while $N_l{}^* = -10^{12}$ cm^{-3}. Assuming the low states to be in partial equilibrium among themselves[1] at an effective excitation temperature T_e, we find $(N_u/g_u)/(N_l/g_l) = 2 \times 10^2$ for Run 5. It should be noted that the measured A_L values are averaged across the jet and local values may be more negative.

Conclusion

Experimental measurements have indicated that a substantial population inversion can be produced in a high-pressure arc heated carbon plasma expanding through a nozzle for the carbon I 2478.6 Å line.

References

[1] Bowen, S. W. and Park, C., "Computer Study of Nonequilibrium Excitation in Recombining Nitrogen Plasma Nozzle Flows," *AIAA Journal*, Vol. 9, No. 3, March 1971, pp. 493–499.

[2] Goldfarb, V. M., Ilina, E. V., Kostygova, I. E., and Lukyanov, G. A., "Spectroscopic Investigation of Supersonic Plasma Jets," *Optics and Spectroscopy*, Vol. 27, 1968, pp. 108–110.

[3] Mitchell, A. and Zemansky, M., *Resonance Radiation and Excited Atoms*, Cambridge University Press, London, 1961, p. 118.

[4] Frish, S. E. and Bochkova, O. P., "Method of Determining Transition Probabilities and Level Population Densities by Self Absorption of Radiation," Rept. AF CRL-63-812, AD 422 515, 1963, Air Force Cambridge Research Lab., Office of Aerospace Research, Bedford, Mass.

[5] Bowen, S. W. and Park, C., "Population Inversion of A.U.V. Atomic Line in Recombining Plasma Nozzle Flow," AIAA Paper 71-592, Palo Alto, Calif., 1971.

[6] Lochte-Holtgreven, W., ed., *Plasma Diagnostics*, North Holland, Amsterdam, 1968, Chap. 2.

[7] Penner, S. S., *Quantitative Molecular Spectroscopy and Gas Emissivities*, Addison Wesley, Reading, Mass., 1959, Chap. 4.

[8] Wiese, W. L., Smith, M. W., and Glennon, B. M., "Atomic Transition Probabilities, Vol. 1, Hydrogen through Neon," National Standard Reference Data Series, National Bureau of Standards 4, 1966.

Dynamical Torsion Theory of Rods Deduced from the Equations of Linear Elasticity

E. J. Brunelle*

Rensselaer Polytechnic Institute, Troy, N.Y.

Introduction

Searching through the last two decades of the literature of mechanics, it is a common occurrence to find the extensional and flexural equations of plates and rods derived by suitably averaging the equations of linear elasticity through the thickness (for plates) or over the cross section (for rods).[1,2] A similar technique for finding the torsional equations of a rod appears to be missing from the literature of mechanics.† The purpose of this Note is to provide such a formulation which is of interest for two reasons. Firstly it is of intrinsic interest to show the intimate relation of the linear equations of elasticity to the dynamical torsion equation and secondly it is of interest to note that, since this technique can be easily extended to average all nonlinear equations of motion, the averaging technique offers a simple alternative to the variational principle as a means of generating approximate equations of motion. This use of the averaging technique has been employed by the author to solve several classes of problems under initial stress and will be the subject of several forthcoming publications.

The present analysis is presented in two parts, the first part being a derivation of the classical torsion equation and the second part being a derivation of the torsion equation with warping effects included.

Mathematical and Physical Preliminaries

Introducing the elastic constants E, $G_{13} = G_{12} = G$, $G_{23} = G_{32} \to \infty$, the warping function $\phi(x_1, x_2, x_3)$, and the twist angle $\theta(x_1, t)$ and assuming the following displacements[4]

$$u_1 = \phi(\partial\theta/\partial x_1) \tag{1}$$

$$u_2 = -x_3\theta \tag{2}$$

$$u_3 = x_2\theta \tag{3}$$

the nonzero strains are given by,

$$\varepsilon_{11} = \partial u_1/\partial x_1 = \partial/\partial x_1(\phi(\partial\theta/\partial x_1)) \tag{4}$$

$$\varepsilon_{12} = \tfrac{1}{2}(\partial u_1/\partial x_2 + \partial u_2/\partial x_1) = \tfrac{1}{2}(\partial\theta/\partial x_1)(\partial\phi/\partial x_2 - x_3) \tag{5}$$

$$\varepsilon_{13} = \tfrac{1}{2}(\partial u_1/\partial x_3 + \partial u_3/\partial x_1) = \tfrac{1}{2}(\partial\theta/\partial x_1)(\partial\phi/\partial x_3 + x_2) \tag{6}$$

and the corresponding stresses‡ are given by,

$$\sigma_{11} = E(\partial/\partial x_1)(\phi(\partial\theta/\partial x_1)) \tag{7}$$

$$\sigma_{12} = G(\partial\theta/\partial x_1)(\partial\phi/\partial x_2 - x_3) \tag{8}$$

$$\sigma_{13} = G(\partial\theta/\partial x_1)(\partial\phi/\partial x_3 + x_2) \tag{9}$$

The equations of linear elasticity

$$\partial\sigma_{ij}/\partial x_i + x_j = \rho\ddot{u}_j \qquad \text{(10a), (10b), (10c)}$$

are now suitably averaged in the two following sections to obtain the desired equations of motion.

Classical Torsion Equation

For the classical case the averaged torque equation is formed by adding the averages (over the cross section) of Eq. (10b) multiplied by $-x_3$ and Eq. (10c) multiplied by x_2. Hence putting Eqs. (2) and (8) into Eq. (10b), multiplying by $-x_3$ and averaging over the cross section (carrying out one integration by parts) yields

$$\frac{\partial}{\partial x_1}\left\{G\frac{\partial\theta}{\partial x_1}\int\!\!\int\left(-x_3\frac{\partial\phi}{\partial x_2} + x_3^2\right)dx_2\,dx_3\right\} - \int_{x_3^-}^{x_3^+} x_3\Big[\sigma_{22}\Big]_{x_2^-}^{x_2^+} dx_3$$
$$- \int_{x_2^-}^{x_2^+}\Big[x_3\sigma_{32}\Big]_{x_3^-}^{x_3^+} dx_2 + \int\!\!\int\sigma_{32}\,dx_2\,dx_3 - \int\!\!\int x_3X_2\,dx_2\,dx_3$$
$$= \ddot{\theta}\int\!\!\int\rho x_3^2\,dx_2\,dx_3 \tag{11}$$

Similarly putting Eqs. (3) and (9) into Eq. (10c), multiplying by x_2 and averaging over the cross section (carrying out one integration by parts) yields

$$\frac{\partial}{\partial x_1}\left\{G\frac{\partial\theta}{\partial x_1}\int\!\!\int\left(x_2\frac{\partial\phi}{\partial x_3} + x_2^2\right)dx_2\,dx_3\right\} + \int_{x_3^-}^{x_3^+}\Big[x_2\sigma_{23}\Big]_{x_2^-}^{x_2^+} dx_3$$
$$- \int\!\!\int\sigma_{23}\,dx_2\,dx_3 + \int_{x_2^-}^{x_2^+} x_2\Big[\sigma_{33}\Big]_{x_3^-}^{x_3^+} dx_2 + \int\!\!\int x_2X_3\,dx_2\,dx_3$$
$$= \ddot{\theta}\int\!\!\int\rho x_2^2\,dx_2\,dx_3 \tag{12}$$

Received August 4, 1971; revision received November 3, 1971.

* Associate Professor of Aeronautics and Astronautics. Member AIAA.

† It must be noted that Warner[3] attempted such a technique in 1965 but his method produced the torsional (shear) wave equation rather than the desired torsional equations of motion.

‡ In general all the stresses are nonzero. However we will need explicit forms for only the stresses given in Eqs. 7, 8, and 9. This is because the other stresses either cancel in pairs in the analysis or appear only in terms evaluated at the boundary.